Magnetoelastic properties and level crossing in $HoVO_4$

P. Morin and J. Rouchy

Laboratoire Louis-Néel, CNRS, 166X, 38042, Grenoble Cedex, France

Z. Kazei

Laboratory for Magnetism, Physics Department, Moscow State University, 119899, Moscow, Russia

(Received 13 July 1994)

The rare-earth oxide compound $HoVO_4$ (tetragonal zircon structure) is investigated in the extended susceptibility formalism, which includes all the features of the crystalline electric field in the analysis of the magnetic, magnetoelastic, and elastic properties as a function of temperature. The characteristic behavior of the first-order magnetic susceptibility allows us to refine the values of the crystalline electric-field parameters and to determine the strength of the magnetic interactions. The magnetoelastic coefficients are then found from third-order magnetic susceptibility, parastriction, and elastic-constants measurements for the different symmetry modes. Their coherency with values determined for $TbPO_4$ is then emphasized: They have the same sign and order of magnitude; in particular the magnetoelastic coefficients for the tetragonal symmetry are sizable in these rare-earth oxides in contrast to the case of rare-earth intermetallics. The unusual temperature dependence of the third-order magnetic susceptibility along the tetragonal axis is a precursor of the level crossing in high magnetic fields associated with a magnetization jump of about $8\mu_B$ at 11.4 T, which we study as a function of temperature down to 0.1 K. The existence of a two-step jump of the magnetization at low temperatures, if not driven by mechanical stresses, remains an intriguing result.

I. INTRODUCTION

$HoVO_4$ belongs to the group of rare-earth (R) oxide compounds RXO_4 $(X = As,P,V)$, which possess a tetragonal zircon structure (space group $I4_1/amd$) at room temperature; the symmetry of the R sites is $42m$.[1] R zircons are known to be archetype Jahn-Teller (JT) compounds, a number of which ($DyVO_4$, $TbVO_4$, $TmVO_4$, $TbPO_4$) exhibit a spontaneous tetragonal-orthorhombic transition.[2] R zircons have several features including their tetragonal local symmetry and the presence of equivalent sites for the R ions, which make them particularly appropriate for theoretical and experimental investigations of the outstanding problems in the sphere of JT interactions. Thanks to their optical transparency, numerous light scattering experiments have been performed, and reliable spectroscopic information is available on the wave functions and energy levels determined by the crystalline electric field (CEF). The magnetic exchange and dipolar interactions are weak (the highest magnetic ordering temperature does not exceed 3.5 K), so that the quadrupolar effects are not overshadowed by the magnetic ordering and quadrupolar orderings may occur in the paramagnetic phase. As a rule, the interaction between JT ions via the long-wavelength acoustic phonons (or strain modes) has been established to prevail for most of the R zircons. The short-range effects are not very important for these systems and the structural phase transitions are described quite perfectly in the mean-field approximation.[2]

Historically the pseudospin formalism, which considers simplified wave functions for only a limited number of low-lying energy levels, has been used to derive the analytical description of the physics. This approach

focuses on the dominant JT mode and fails to explain the detailed behavior due to CEF peculiarities or less active JT modes. It does not permit one to trace the variation of the interaction constants through the R zircon series nor give a full knowledge of the JT couplings.

More recently, an extended magnetic and quadrupolar susceptibility formalism based on the actual wave functions and level energies has been successfully applied to study the quadrupolar interactions in a large number of R intermetallics with cubic and tetragonal structures.[3-6] This approach, based on perturbation theory in the disordered phase, allows one to determine for all the symmetry modes both the one-ion magnetoelasticity and the quadrupolar pair interactions, starting from the ordinary (magnetic, magnetoelastic, and elastic) experimental data. The knowledge of these different couplings combined with self-consistent diagonalization of the full Hamiltonian then allows the properties in the ordered phase or in high magnetic fields to be determined.[6]

We here propose an application of this susceptibility formalism to $HoVO_4$. The procedure follows that was used previously for $TbPO_4$, another complicated system,[7] and will allow a preliminary comparison of magnetoelastic couplings between the R vanadates and phosphates. In $HoVO_4$, the JT interactions are not large enough to drive a quadrupolar ordering, but nevertheless give sizable effects. According to the spectroscopic investigations of $HoVO_4$,[8] the ground multiplet $^5I_8$ of the Ho^{3+} ion splits in the tetragonal crystal field into a Γ_1 singlet, a Γ_5 doublet at 21 cm^{-1} above, and a Γ_4 singlet accidentally degenerate with a second Γ_5 doublet at 47 cm^{-1}. The first excited doublet at 21 cm^{-1} in the concentrate system $HoVO_4$ shows clearly a small zero-field splitting of about

(2.3 ± 0.1) cm^{-1} at temperatures lower than 20 K. This splitting seems to be due to some cooperative effect since it is not present in dilute system $Ho_{0.1}Y_{0.9}VO_4$. Furthermore a number of different experiments have so far failed to reveal evidence for any corresponding static symmetry lowering: the splitting of this excited doublet has thus been assumed to be dynamic or to result from an artifact of the optical absorption spectrum.[9]

Another interesting result from the light scattering studies is the dependence of the low-lying levels in a high magnetic field applied along the c axis.[8,9] Indeed a crossing is observed at around 12 T between the Γ_1 singlet, which remains field independent and a sublevel of the Γ_5 doublet. A strong (~175) enhancement of the effective nuclear moments of the Ho ions in the (001) plane is associated with Van Vleck behavior at low temperature,[10] so that $HoVO_4$ is a suitable candidate for enhanced nuclear cooling experiments.[11] Magnetic susceptibility following demagnetization cooling reveals that the hyperfine enhanced nuclear moments of ^{165}Ho antiferromagnetically order at about 4.5 mK.[12−14]

The temperature dependence of some elastic constants measured below 250 K indicate that they contain sizable magnetoelastic contributions, which drive a softening of about 11 and 6 % for the γ and δ elastic modes around 15 K, which stiffen at still lower temperatures towards a Van Vleck plateau.[15] This corresponds to a transfer of population from the quadrupolar Γ_5 doublet in favor to the nonquadrupolar Γ_1 singlet. The nondivergence of the associated strain susceptibilities clearly agrees with the absence of a spontaneous quadrupolar ordering.

Thus though, at first sight, $HoVO_4$ is not dominated by strong JT correlations as, for example, in $TbVO_4$, $DyVO_4$, and $TmVO_4$, it exhibits several features that are not adequately explained and it appears to us a good candidate for a reinvestigation using the susceptibility formalism. After a brief recall of this treatment in the following section, we analyze the CEF properties in Sec. IV. The magnetic, magnetoelastic properties, and the level crossing induced by a magnetic field applied along the c axis are discussed in Sec. V. A comparison with $TbPO_4$ is then given in Sec. VI.

II. FORMALISM

The magnetic properties of the $4f$ shell are described with the following Hamiltonian using the equivalent operator method[16] and the mean-field approximation (MFA):[4,7]

$$\mathcal{H}=\mathcal{H}_{CEF}+\mathcal{H}_M+\mathcal{H}_{ME}+\mathcal{H}_Q+E_{el}+E_M+E_Q \ . \quad (1)$$

The CEF term, $\mathcal{H}_{CEF}$, is written within a system of x,y,z axes parallel to the [100], [010], and [001] axes of the lattice cell, respectively,

$$\mathcal{H}_{CEF}=\alpha_J V_2^0 O_2^0+\beta_J(V_4^0 O_4^0+V_4^4 O_4^4)+\gamma_J(V_6^0 O_6^0+V_6^4 O_6^4) \ , \quad (2)$$

O_l^m are the Stevens operators, V_l^m the CEF parameters, α_J, β_J, γ_J the Stevens coefficients. The magnetic terms in $\mathcal{H}_M$ are the Zeeman coupling to the applied magnetic field, H, corrected for demagnetizing effects and the Heisenberg-type bilinear interactions, characterized by a θ^* magnetic interaction temperature. Only magnetoelastic contributions linear in strain and restricted to second-rank terms are considered here. They read in symmetrized notation as[17]

$$\mathcal{H}_{ME}=-(B^{\alpha1}\varepsilon^{\alpha1}+B^{\alpha2}\varepsilon^{\alpha2})O_2^0-B^{\gamma}\varepsilon^{\gamma}O_2^2$$
$$-B^{\delta}\varepsilon^{\delta}P_{xy}-B^{\varepsilon}(\varepsilon_1^{\varepsilon}P_{zx}+\varepsilon_2^{\varepsilon}P_{yz}) \quad (3)$$

with $P_{ij}=\frac{1}{2}(J_iJ_j+J_jJ_i)$ $(i,j=x,y,z)$ (see also Ref. 3). The B^{μ}'s are the magnetoelastic coefficients, which are temperature independent. The related elastic energy is

$$E_{el}=\frac{1}{2}C_0^{\alpha1}(\varepsilon^{\alpha1})^2+C_0^{\alpha12}\varepsilon^{\alpha1}\varepsilon^{\alpha2}+\frac{1}{2}C_0^{\alpha2}(\varepsilon^{\alpha2})^2$$
$$+\frac{1}{2}C_0^{\gamma}(\varepsilon^{\gamma})^2+\frac{1}{2}C_0^{\delta}(\varepsilon^{\delta})^2+\frac{1}{2}C_0^{\varepsilon}[(\varepsilon_1^{\varepsilon})^2+(\varepsilon_2^{\varepsilon})^2] \ . \quad (4)$$

The ε^{μ} strains and the C_0^{μ} lattice background elastic constants are given in Refs. 4 and 7. Within the MFA, the two-ion quadrupolar terms are written as

$$\mathcal{H}_Q=-K^{\alpha}\langle O_2^0\rangle O_2^0-K^{\gamma}\langle O_2^2\rangle O_2^2-K^{\delta}\langle P_{xy}\rangle P_{xy}$$
$$-K^{\varepsilon}\{\langle P_{yz}\rangle P_{yz}+\langle P_{zx}\rangle P_{zx}] \ . \quad (5)$$

E_Q and E_M in Eq. (1) are the quadrupolar and bilinear corrective energies associated to the MFA. Minimizing the free energy with regard to the strains gives the equilibrium strains as functions of the expectation values of the corresponding quadrupolar operators. Replacing these ε^{μ}'s makes $\mathcal{H}_{ME}$ [Eq. (3)] indistinguishable from $\mathcal{H}_Q$ [Eq. (5)] and leads to total quadrupolar coefficients:

$$G^{\mu}=\frac{(B^{\mu})^2}{C_0^{\mu}}+K^{\mu} \quad (\mu=\gamma,\delta,\varepsilon) \quad (6)$$

and

$$G^{\alpha}=\frac{(B^{\alpha1})^2C_0^{\alpha2}-2B^{\alpha1}B^{\alpha2}C_0^{\alpha12}+(B^{\alpha2})^2C_0^{\alpha1}}{C_0^{\alpha1}C_0^{\alpha2}-(C_0^{\alpha12})^2}+K^{\alpha} \ . \quad (6')$$

In insulating systems, the two-ion quadrupolar terms originate essentially from phonon couplings.[2] In the presence of only acoustic phonon exchange, the pair interaction coefficient K^{μ} is negative and a relation is expected between K^{μ} and the magnetoelastic contribution to G^{μ}, $G_{ME}^{\mu}=(B^{\mu})^2/C_0^{\mu}$:

$$K^{\mu}/G_{ME}^{\mu}=-\frac{1}{3} \ .$$

This ratio is close to that observed, for instance, in $TmVO_4$, and appears as a general feature for rare-earth zircons.[2,18,19]

In the presence of small external stresses, perturbation theory can be applied very fruitfully to the disordered phase. It is then possible to obtain analytical expressions for the free energy associated with each of the symmetry lowering modes and then to describe the corresponding couplings.[4] For example, the third-order magnetic susceptibility, i.e., the coefficient of the H^3 term in the field expansion of the magnetization reads as

$$\chi_M^{(3)} = \frac{1}{[1-(\theta^*/C)\chi_0]^4}\left[\chi_0^{(3)} + \frac{2G^\alpha(\chi_\alpha^{(2)})^2}{1-G^\alpha\chi_\alpha} + \frac{2G^\mu(\chi_\mu^{(2)})^2}{1-G^\mu\chi_\mu}\right].$$ (7)

Only the α mode is present for H parallel to the [001] axis with the γ and δ modes active for H along the [100] and [110] directions, respectively. χ_0 is the first-order susceptibility, which is anisotropic between the [001] axis and the basal plane. Three anisotropic single-ion susceptibilities are introduced, which are known as soon as the CEF is determined: $\chi_0^{(3)}$ describes the initial curvature of the magnetic response in the absence of any magnetic interaction. The strain susceptibility, $\chi_\mu = \partial\langle O_2^\mu\rangle/\partial\varepsilon^\mu$, is responsible of the softening of the associated elastic constant,

$$C^\mu = C_0^\mu - \frac{(B^\mu)^2\chi_\mu}{(1-K^\mu\chi_\mu)}.$$ (8)

$\chi_\mu^{(2)} = \partial\langle O_2^\mu\rangle/\partial H^2$ is the quadrupolar response to a magnetic field and determines the parastriction: the strain includes the renormalization of the applied field by the bilinear interactions and of the quadrupolar response by the quadrupolar pair interactions:

$$\varepsilon^\mu = \frac{B^\mu}{C_0^\mu}\frac{\chi_\mu^{(2)}}{(1-n\chi_0)^2(1-G^\mu\chi_\mu)}H^2.$$ (9)

Each of the ε^μ's can be determined from the combinations of $\lambda_{\alpha_1\alpha_2\alpha_3}^{\beta_1\beta_2\beta_3}$ changes of length induced by a $(\alpha_1\alpha_2\alpha_3)$ magnetic field and measured in appropriate $(\beta_1\beta_2\beta_3)$ directions. Extensive applications of the susceptibility formalism in tetragonal symmetry can be found in Ref. 6 for TmAg₂. After the determination of the CEF and of the single-ion susceptibilities, the fit of the first-order magnetic susceptibility along the [001] axis and in the basal plane provides us with the bilinear temperature, θ^*. The other experiments (third-order susceptibility, elastic constant, and parastriction) give the different pairs of B^μ and K^μ coefficients.

III. SAMPLES AND EXPERIMENTAL TECHNIQUES

The well-known method of spontaneous crystallization from solution was used to grow the single crystals of HoVO₄ with molten PbO-PbF₂-V₂O₅-H₃BO₃ as the solvent. The crystals were transparent and slightly colored, their length was about 2 or 3 mm in each direction of the crystallographic cell. The magnetization measurements were performed using two different magnetometers in steady magnetic fields up to 80 and 160 kOe. The temperature ranges were 1.6–300 K and 0.05–1.6 K for the He³-He⁴ dilution refrigerator. The temperature was regulated within ±0.01 K and the accuracy of the magnetization was around $0.02\mu_B$. Magnetostriction deformation was measured by resistive strain gauges both parallel and perpendicular to the external magnetic field, which pointed along one of the principal symmetry axes of the crystal. The absolute accuracy of the magnetostriction

measurements was about 2×10^{-7} in the liquid-helium temperature range and 10^{-6} at high temperatures.

IV. THE CRYSTALLINE ELECTRIC FIELD

Since the exact knowledge of the CEF is a prerequisite to the use of the susceptibility formalism, we tried to improve its determination for HoVO₄. Previous studies in the literature give somewhat different sets of CEF parameters. In addition to the studies of Battison et al.[8] and Bleaney et al.,[9] CEF parameters were derived from the absorption spectra investigations in the near-infrared region by Bischoff et al.[20] Table I shows that both sets of parameters are relatively close to each other. Andronenko et al.[21] used the CEF parameters found for Er³⁺ in YVO₄ multiplied by a factor of 1.2. As indicated in Ref. 9, the parameters from Goto are different and not mutually consistent.[15]

Thus, to our knowledge, there exist at least four different sets of crystal-field parameters which each describe more or less correctly one type of experiment. To improve the determination of the CEF parameters, we used our magnetic susceptibility data together with the spectroscopic results.

A. Magnetic susceptibility measurements

Isothermal magnetization curves were collected along the [001], [100], and [110] directions in fields up to 76 kOe and temperatures ranging from 1.5 to 300 K. Additional measurements were performed also with a He³-He⁴ dilution refrigerator in temperatures down to 100 mK. The first-order magnetic susceptibility was deduced from the M/H versus H^2 plots; the zero-field extrapolation of these plots provides us with the magnetic susceptibility, the initial slope with the third-order component. Magnetic susceptibility in the basal plane is isotropic within the experimental accuracy. A large anisotropy of the first-order susceptibility is observed in favor of the basal plane, in particular at low temperature. Measurements of the weak signal along the c axis are delicate: CEF calculations have shown that, below 5 K, a 1° or 2° misalignment of the external magnetic field out of the [001] axis leads to a contribution from the basal plane comparable with the c-axis magnetic susceptibility. Sequences of measurements on four different samples gave reciprocal susceptibility values ranging at low temperature from 400 to 600 kOe/μ_B; only the sequence giving the smallest susceptibility will be considered in the following.

The temperature variation of the reciprocal susceptibility is drawn in Fig. 1. Above 100 K, the variation is close to a Curie-Weiss law, with slightly different slopes along the c and a axes, which indicates that CEF effects are still present at room temperature. As temperature decreases,

TABLE I. CEF parameters from the literature.

	V_2^0 (K)	V_4^0 (K)	V_4^4 (K)	V_6^0 (K)	V_6^4 (K)
Ref. 9	−127	57	−1114	−61	112
Ref. 20	−131	66	−1087	−65	132
Ref. 21	−173	73	−1395	−72	151
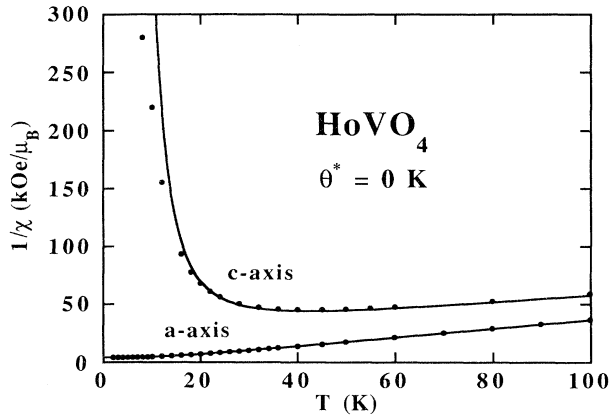
FIG. 1. The temperature dependence of the reciprocal first-order susceptibility along the [100] and [001] axes (data, solid dots) in HoVO₄. The lines are variations calculated without bi-linear interactions.

the magnetic susceptibility in the basal plane increases monotonically, whereas, along the tetragonal axis, it exhibits a broad maximum around 40 K and decreases rapidly at lower temperatures resulting in a huge anisotropy of about 150. In both directions, a Van Vleck behavior is observed at low temperature in agreement with the non-magnetic nature of the ground-state singlet. The reciprocal magnetic susceptibility at low temperature in the basal plane, $\chi_{[100]}^{-1}$ (2 K)=4.33 kOe/μ_B, is very close to the value estimated from the enhanced nuclear frequency of a Ho^{3+} ion in the perpendicular plane [4.312(2) kOeμ/B].[9]

B. The crystalline-electric-field parameters

In order to describe our magnetic susceptibility data, we took the CEF parameters in Table I as a starting point for a self-consistent diagonalization of $\mathcal{H}_{CEF}+\mathcal{H}_M$ by a least-squares procedure which searches for minimums in the residue in the space of the V_1^m's.[5] The parameters of Ref. 21 lead to the largest residue. The sets from Refs. 9 and 20 gave fits clearly better and of similar quality; the optimum fit to our magnetic data (Fig. 1) is obtained with $V_2^0=-126$ K, $V_4^0=55$ K, $V_4^4=-1105$ K, $V_6^0=-62$ K, and $V_6^4=112$ K, a set very close to the one proposed by Bleaney.[9] The uncertainties associated with the parameters are small, around 1 or 2 K (5 K for V_4^4). Note that below 5 K, the susceptibility calculated along the c axis is systematically smaller than the experimental one which indicates a slight misorientation of the sample and introduces a contribution to the measured value from the basal plane. In addition to the temperature dependences of the susceptibility, this set of V_m^l closely describes the light scattering data and the enhanced nuclear magnetic properties.[9] It will be kept constant in the following. Bi-linear interactions are very small. Therefore, the θ^* bi-linear exchange temperature will be taken as zero in the following.

V. MAGNETIC AND MAGNETOELASTIC PROPERTIES

A. Third-order magnetic susceptibility

The third-order magnetic susceptibility along the c axis (upper part of Fig. 2) is positive over the entire investigated temperature range; it is null at low temperature, passes by a maximum around 16–20 K and decreases at higher temperatures. Also shown in Fig. 2 is the variation calculated when considering only the CEF. Despite the weakness of $\chi_M^{(3)}$ along the c axis compared to its values in the basal plane (lower part of Fig. 2) and the possible parasitic contributions due to misalignments this implies the agreement is reassuringly good in particular near the maximum value. The discrepancy between calculated and measured $\chi_M^{(3)}$ values at the maximum is in the range of the absolute uncertainty in the present experiment (around $0.5\times10^{-6}\mu_B$/kOe^3).

The Van Vleck behavior is a direct consequence of the nonmagnetic nature of the ground-state singlet;[4] the almost zero value at 0 K results essentially from the fact that the $|0\rangle$ component in the $|J_Z\rangle$ basis makes up 95% of the ground-state wave function. Its other $|\pm4\rangle$ and $|\pm8\rangle$ components are small and lead to couplings between the ground-state singlet and the high excited singlets at 330 and 380 K, the algebraic sum of which according to Eq. (A9) in Ref. 4 is very weak. The peak around 15 K is driven by the increased population of the first excited doublet lying at 31 K. Such a situation was
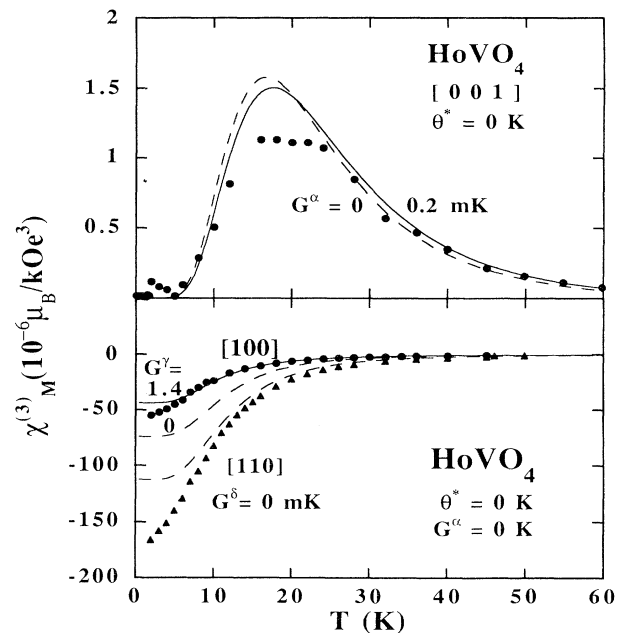
FIG. 2. The temperature variation of the third-order susceptibility along the [001] axis (upper part, dots), the [100] axis (dots), and the [110] axis (triangles). The dashed curves are calculated with only the crystalline-electric-field contribution, the solid curves result from calculations also including quadrupolar contributions as indicated.

predicted in Ref. 4, but has been never observed. For a magnetic field along the c axis, the third-order susceptibility may be marked by quadrupolar interactions within the α symmetry only. Contrary to the case of TbPO$_4$,[7] their inclusion in the calculations does not improve the fit as will be discussed later.

A similar study was performed in the basal plane for a magnetic field applied along [100] and [110] directions (lower part of Fig. 2). The third-order magnetic susceptibility is negative and anisotropic; the absolute value for the [110] direction is three times larger than that for [100], which indicates that the easy magnetization direction is the [100] axis. Along the [110] axis, $\chi_M^{(3)}$ calculated without any quadrupolar and bilinear interactions, i.e., $\chi_0^{(3)}$, does not closely describe the data. However considering δ quadrupolar interactions does not strongly change the calculated dependence owing to the small values of the δ susceptibilities present in Eq. (7). We have to note the fit here is worse than usually observed in R intermetallics such as TmAg$_2$.[6] Along the [100] axis, the shift between $\chi_M^{(3)}$ and $\chi_0^{(3)}$ vanishes if the latter is renormalized by quadrupolar terms with a G^γ coefficient of 1.4 mK. A small discrepancy is still present below 5 K, the origin of which is unexplained. The shift of $\chi_M^{(3)}$ towards positive values due to γ quadrupolar terms increases then the anisotropy in the basal plane in favor of the [100] axis.

B. Parastriction

To obtain all the magnetostrictive modes the changes of length parallel and perpendicular to the magnetic field directed along the [001], [100] and [110] axes have been measured in isothermal conditions. The change of length was always quadratic in the applied field, for temperatures above 20 K up to 50 kOe and, for lower temperatures up to fields of 10 kOe at least for the easy magnetization direction.

1. α mode

The magnetic field was applied along the [001] axis, the changes of length, $\lambda_{[001]}$ and $\lambda_{[100]}$, lead to the tetragonal symmetry modes $\varepsilon^{\alpha 1} = \lambda_{[001]} + 2\lambda_{[100]}$ and $\varepsilon^{\alpha 2} = \lambda_{[001]} - \lambda_{[100]}$. According to Eq. (9), the temperature variations may be linearized, at least at high temperature, by plotting $H/|\lambda_{[001]} + 2\lambda_{[100]}|^{1/2}$ and $H/|\lambda_{[001]} - \lambda_{[100]}|^{1/2}$ as done in Fig. 3. The accuracy of the measurements is higher for the $\varepsilon^{\alpha 2}$ mode than for the $\varepsilon^{\alpha 1}$ mode since systematic errors cancel in the first case. However, both modes display the same temperature variation with a vanishing of the strain at low temperature. Indeed in the absence of bilinear interactions, the calculated behaviors are given by[4,7]

$$(3/2)^{1/4}\sqrt{|A^{\alpha 2}|}H/\sqrt{|\varepsilon^{\alpha 2}|} = (3)^{1/4}\sqrt{|A^{\alpha 1}|}H/\sqrt{|\varepsilon^{\alpha 1}|}$$

$$= 1/\sqrt{|\chi_\alpha^{(2)}|}(1 - G^\alpha\chi_\alpha)^{1/2} .$$

(10)

$A^{\alpha 1}$ and $A^{\alpha 2}$ depend on both the background elastic con-
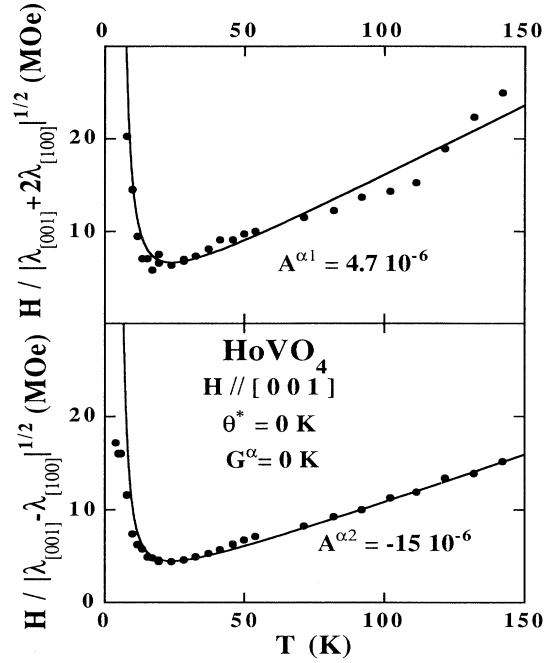
FIG. 3. The temperature variation of the parastriction within the α tetragonal symmetry for a [001] magnetic field (upper part, $\alpha 1$ mode; lower part, $\alpha 2$ mode). The solid curves are calculated dependences.

stants and the magnetoelastic coefficients, $B^{\alpha 1}$ and $B^{\alpha 2}$:

$$A^{\alpha 1} = \frac{B^{\alpha 1}C_0^{\alpha 2} - B^{\alpha 2}C_0^{\alpha 12}}{C_0^{\alpha 1}C_0^{\alpha 2} - (C_0^{\alpha 12})^2}$$

and

$$A^{\alpha 2} = \frac{B^{\alpha 2}C_0^{\alpha 1} - B^{\alpha 1}C_0^{\alpha 12}}{C_0^{\alpha 1}C_0^{\alpha 2} - (C_0^{\alpha 12})^2} .$$

The fit to the data leads to $A^{\alpha 1}$ and $A^{\alpha 2}$ values given in Fig. 3. Note that the negative sign observed for $\varepsilon^{\alpha 2}$ corresponds to a negative value of $A^{\alpha 2}$ since $\chi_\alpha^{(2)}$ is calculated to be positive. Introducing G^α values in Eq. (10) is not necessary. In order to determine $B^{\alpha 1}$ and $B^{\alpha 2}$, we use the values of the elastic constants from Ref. 15. The hypothesis of $C_{13} = C_{12}$ leads to the symmetrized elastic constants $C_0^{\alpha 1} = 24$, $C_0^{\alpha 2} = 11$, and $C_0^{\alpha 12} = 1.6$ in 10^5 K units. We obtain $B^{\alpha 1} = 9$ K and $B^{\alpha 2} = -15$ K and then a magnetoelastic contribution $G_{\text{ME}}^\alpha = 0.26$ mK [Eq. (6')]. As discussed in Refs. 4 and 7, the existence of α magnetoelastic couplings acting on the nonzero $\langle O_2^0 \rangle$ quadrupolar component, already ordered by the CEF, has to be considered ab $initio$ in the diagonalization of the starting hamiltonian. We have checked that a G^α value around 0.2 mK does not drastically change either the single-ion susceptibilities themselves or the fits (see, for instance, in Fig. 2 the effect of G^α on $\chi_M^{(3)}$ along the c axis). As the modification (in general an improvement) of the fits is less than 3%, the effect of the α quadrupolar pair interactions will be not considered in the following ($G^\alpha = 0$ K).

P. MORIN, J. ROUCHY, AND Z. KAZEI

2. δ and γ modes

Owing to the singlet ground state, the orthorhombic symmetry modes exhibit a Van Vleck-type behavior at low temperature. Over all the temperature range investigated, $\varepsilon^\delta = \lambda_{[110]} - \lambda_{[-110]}$ and $\varepsilon^\gamma = \lambda_{[100]} - \lambda_{[010]}$ are positive and negative, respectively. The temperature variations of the reciprocal parastriction are given in Fig. 4. Since the quadrupolar field susceptibilities, $\chi_\mu^{(2)}$, are positive, the two magnetoelastic coefficients are of opposite sign. The adjustments of the experimental and calculated behaviors leads to $B^\delta = 54$ K and $B^\gamma = -30$ K for background elastic constants,[15] $C_0^\delta = 19.5 \times 10^4$ K and $C_0^\gamma = 96 \times 10^4$ K, respectively. The following values are then deduced for the magnetoelastic contributions: $G_{ME}^\delta = 15$ mK and $G_{ME}^\gamma = 0.9$ mK. For the δ symmetry mode, as observed for the third-order susceptibility, the parastriction does not strongly depend on quadrupolar pair interactions and, here too, it is not possible to directly determine the G^δ value with accuracy. To the contrary, the presence of a G^γ contribution introduces a shift of the calculated behavior (low part of Fig. 4) and a value of G^γ around 1 mK agrees with the determination from the third-order susceptibility (Sec. V A).

C. Elastic constants

The above determinations have been completed by the analysis of the elastic constants measured by Goto et al.[15] The $C^\gamma = C_{11} - C_{12}$, $C^\delta = 2C_{66}$ and $C^\varepsilon = 2C_{44}$ normal elastic modes were measured below 250 K. As indicated by the authors, the data around this temperature seem to be questionable. The thermal variation of the C^ε mode is very similar to the background lattice contribution, which indicates a nonmeasurable B^ε magnetoelastic coefficient in agreement with our parastriction measure-

ments. For C^γ and C^δ, a minimum is observed around 15 K and the softening reaches 11 and 6 % of the maximum value, respectively.
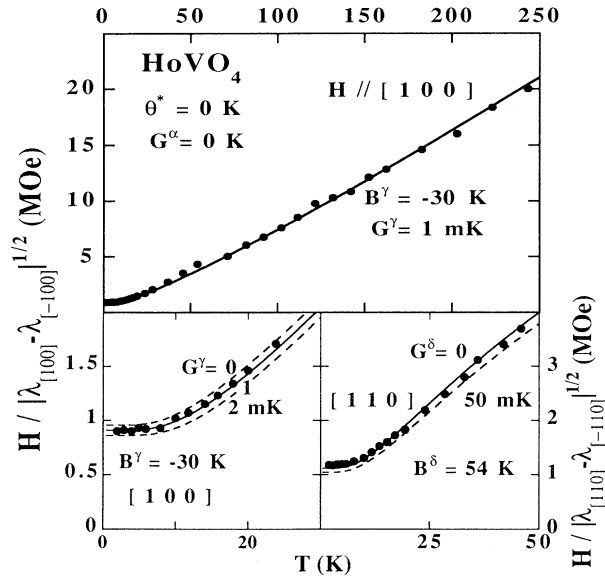
The best fit of the temperature dependence of C^γ is obtained with the absolute value $|B^\gamma| = 33.5$ K for the magnetoelastic constant, and a quadrupolar pair coefficient $K^\gamma = -0.3$ mK (Fig. 5). The values deduced, $G_{ME}^\gamma = 1.2$ mK and $G^\gamma = 0.9$ mK, are in full agreement with determinations from the third-order susceptibility and parastriction. For the δ symmetry, a worse fit to the C^δ data is obtained, in particular above 100 K, where some spurious contributions are believed to take place. The $|B^\delta|$ absolute value (around 85 K) is clearly larger than the one determined by parastriction, as will be discussed in the conclusion.

D. Level crossing

The very small first- and third-order magnetic susceptibilities observed along the c axis in Secs. IV A and V A indicate that the ground-state energy is not shifted with field at low temperature. The condition for the existence of a crossing with an excited magnetic level in a realizable magnetic field can be fulfilled only if the magnetic excited level is not too energetic. This is the case in HoVO$_4$ around 11 T as observed by spectroscopic investigations of the Zeeman effect: the ground-state singlet shows little magnetic field dependence whereas the first and especially the second excited doublets at 31 and 66 K split significantly. The wave function of the new ground state above the crossing has a dominant $|7\rangle$ component as the second excited doublet in zero magnetic field.[8,9] To study the crossing and the induced magnetic moment as functions of temperature, magnetization measurements have been performed in magnetic fields up to 15 T applied along the c axis.

Examples of isothermal magnetization curves are reported in Fig. 6 for different temperatures. It is seen that the low-temperature magnetization is very small below 10 T and rapidly increases at the critical field of 11.4 T. Above this, the magnetization saturates at the value of $8.2\mu_B$. The magnetization jump becomes sharper as the

FIG. 4. The temperature dependence of the parastriction for the γ and δ orthorhombic symmetries. Curves are calculated with the parameters indicated.
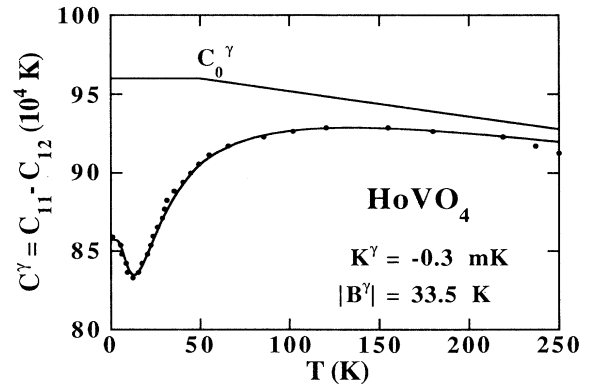
FIG. 5. The temperature dependence of the C^γ elastic constant. The data are from Ref. 15. The curve is calculated with the parameters indicated.
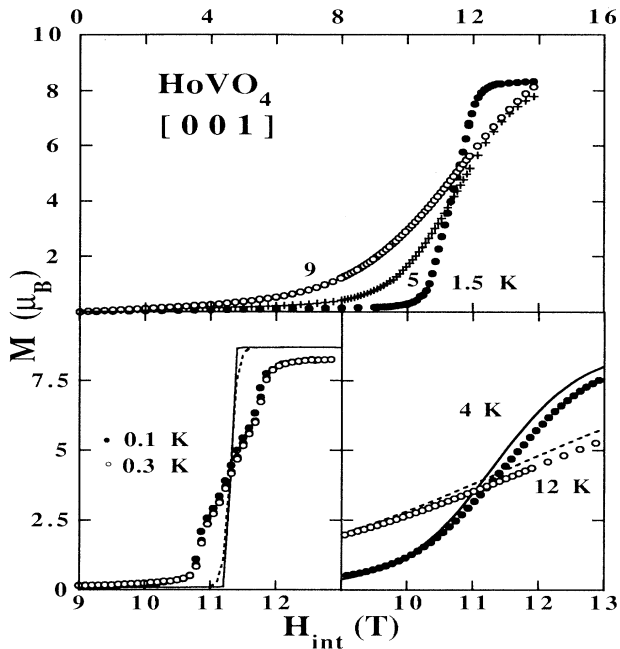
FIG. 6. Isothermal magnetization curves along the c axis, the applied field is corrected for demagnetizing effects. The dashed and solid curves are calculated in the presence of only the crystalline electric field at 0.3, 12 K and 0.1, 4 K, respectively.

FIG. 7. The field derivative of the isothermal magnetization as a function of the internal field. The solid curves are calculated in the presence of only the crystalline electric field. Each variation is vertically shifted as indicated in parentheses.

temperature decreases down to 1.5 K, whereas the critical field corresponding to the inflection point does not change noticeably. The hysteresis between the variations of the magnetization in increasing and decreasing fields is small, less than 1 kOe. Below 1.5 K, two different steps are clearly observed with a linear magnetization dependence in between. Thus the width in field of the transition never decreases to less than 1.5 T.

Above 3 K, the curves calculated with the same set of CEF parameters and coupling constants as previously, describe the experimental ones except that the magnetization calculated above the critical field is overestimated by 0.2μ_B and the calculated magnetization slope at the crossing is slightly too high (Figs. 6 and 7). Including antiferromagnetic interactions reduces the value of the field felt by a given 4f ion in the paramagnetic state and a value θ^* about -1 K, sufficiently small not to affect the measurements of Sec. IV B, would remove the gap between the experiment and calculation. It would not reduce sizably the magnetization calculated in high fields. However we have checked that the diminution of the calculated slope by the negative bilinear interactions would be compensated by considering the $G^\alpha = 0.2$ mK contribution, which acts in sense of increasing the slope.

Thus the width in field of the transition cannot be explained by this way. This is due to the double profile of the experimental transition. Below 3 K, the resolution into two steps is well emphasized by the two peaks in the derivative, split symmetrically with respect to the unique calculated peak, which becomes narrower and narrower (0.2 T at 0.1 K), according to the thermal depopulation of the upper level on both sides of the crossing (Fig. 8). Note that the peaks have, in the limits of the experimen-

tal accuracy, a width and a thermal variation of the same order as the calculated one. The double transition may result from mechanical stresses. Because of the torque in high magnetic fields applied along the hard axis, we failed to measure the magnetization in a free sample, which had to be inserted into a drop of epoxy to prevent it from breaking. At the critical field, sizable magnetostriction changes occur: on both sides of the magnetization jump, the quadrupolar components are calculated to be $\langle O_2^0 \rangle = 74$ (high magnetization state) and -67 (low magnetization state) and the free energy at 0.1 K changes at the critical field by 1.56 K for $G^\alpha = 0.2$ mK. The variation of the quadrupolar component $(\Delta\langle O_2^0 \rangle = 141)$ and
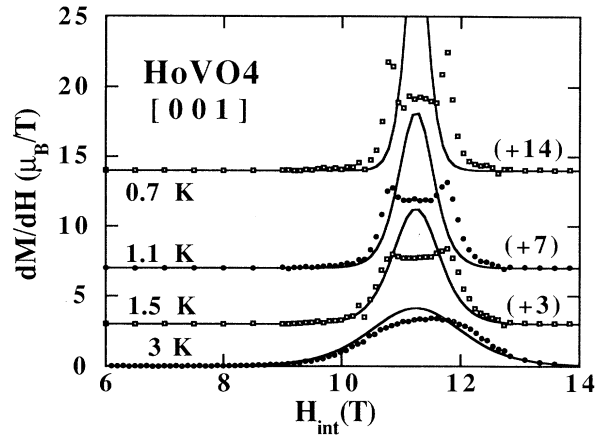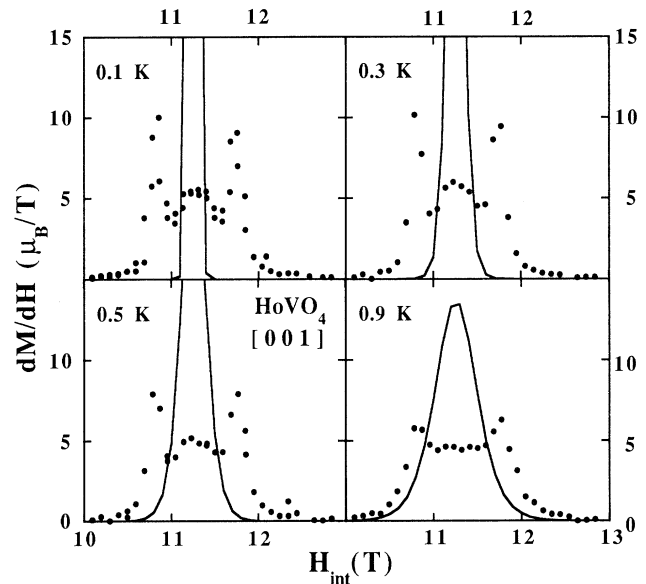
FIG. 8. The field derivative of the magnetization as a function of the internal field at low temperatures. The solid curves are calculated in the presence of only the crystalline electric field.

the magnetoelastic coefficients $B^{\alpha 1}$ and $B^{\alpha 2}$ determined by parastriction give the magnetostrictive changes $\Delta\varepsilon^{\alpha 1}=0.66\times 10^{-3}$ and $\Delta\varepsilon^{\alpha 2}=-2.12\times 10^{-3}$, which implies $\Delta\lambda_{[001]}=-1.35\times 10^{-3}$ and $\Delta\lambda_{[100]}=1.25\times 10^{-3}$. These deformations may give rise to strong and inhomogeneous stresses in the clamped sample and thus be responsible for the double feature of the transition at low temperatures. However, if not fortuitous, the symmetrical shape of the magnetization curve as well as of its field derivative is surprising and there may exist other explanations (see discussion).

VI. DISCUSSION

Our susceptibility measurements have confirmed the CEF parameters proposed in Ref. 9. They also show the bilinear interactions between magnetic moments to be weak. In the paramagnetic range, they are characterized by a θ^* temperature slightly negative ranging from 0 to a minimum of -2 K. This agrees with the magnitudes of the Néel temperature in isomorphous compounds (for instance, 3.5 K in $DyVO_4$).

The magnetoelastic couplings associated with the α tetragonal symmetry (change of the c/a ratio and change of the volume) are sizable, although weaker than in $TbPO_4$.[7] Their consequences have been found to be quite important in $TbPO_4$ due to the close vicinity of the low-lying levels. In $HoVO_4$ they are not as drastic owing to the large spacings (31 and 66 K for the first two excited levels) and may be neglected in the fit of all the other properties. With the assumption of $C_{13}=C_{12}$, the magnetoelastic coefficients $B^{\alpha 1}=9$ K and $B^{\alpha 2}=-15$ K have been determined. As for all the magnetoelastic coefficients, $B^{\alpha 1}$ and $B^{\alpha 2}$ are simply the strain derivatives of the second-order CEF parameter.[3] They thus behave as any CEF parameter and after normalization by the second-order Stevens coefficient, may be compared from one compound to the other or from one series to another isomorphous one. In $HoVO_4$, the following ratios are obtained: $B^{\alpha 1}/\alpha_J=-4050$ and $B^{\alpha 2}/\alpha_J=6300$ K, reminiscent of values -7000 and 4600 K obtained in $TbPO_4$. These values are about 20 or 50 times larger than in tetragonal $R Ag_2$.[6] The quite sizable magnitude of these α magnetoelastic modes seems to be general to the R zircons, contrary to the case of R intermetallics, for which the α modes are dominated by the symmetry-lowering modes.[3]

For symmetry-lowering modes, the normalization by the Stevens coefficient of the magnetoelastic coefficients, $B^{\delta}=54$ K and $B^{\gamma}=-30$ K, leads to $B^{\delta}/\alpha_J=-24\,300$ and $B^{\delta}/\alpha_J=13\,500$ K, compared to $-14\,400$ and 9900 K in $TbPO_4$. For each mode, the sign is the same for both compounds and the absolute values are not very different, although the magnetoelastic coefficients for the symmetry lowering modes appear larger in RVO_4 (preliminary results in other isomorphous systems confirm this tendency). This latter feature supports the more frequent occurrence of structural transitions in the second series, although it is not the main reason: the ground state and low-lying levels exhibit intrinsic quadrupolar components

more often in RVO_4 than in RPO_4. This is in particular due to the fact that, whereas the fourth- and six-order CEF coefficients are similar, the large second-order ones, V_2^0, are of opposite sign,[20] which reverse the order of the CEF levels. Thus changing V to P inside the oxygen cages of the zircon cell strongly modifies the V_2^0 coefficient, but not its strain derivatives, which are observed here to behave as the fourth and sixth-order CEF coefficients. Systematic determinations across the two series will allow us to state this result precisely. When confirmed, this will give a general model for all the R zircons governed by the CEF and its magnetoelastic modulation.

The determinations of the magnetoelastic couplings, in particular for the γ symmetry, are coherent between the various experimental probes. The total quadrupolar coefficient G^{γ} ranges from 1.4 to 0.9 mK, its magnetoelastic contribution, G_{ME}^{γ}, from 0.9 to 1.2 mK. The best-fit parameters for the temperature variation of the elastic mode C^{γ} lead to quadrupolar pair interactions, which have a $-\frac{1}{3}$ ratio with respect to the magnetoelastic contribution, as expected in the case of an acoustic phonon coupling.[2] However some shifts from this theoretical value to account for particular experimental conditions are possible as it can be deduced from the parastriction values ($G^{\gamma}=1$, $G_{GE}^{\gamma}=0.9$ mK). A similar analysis is not possible for the δ symmetry due to the small quadrupolar susceptibilities, which limit the experimental sensitivity and accuracy: the temperature variation of both the third-order susceptibility and the parastriction does not lead to a well-defined G^{δ} value. From the magnetoelastic coefficient, $B^{\delta}=54$ K, deduced from the parastriction, the magnetoelastic contribution is estimated as $G_{ME}^{\delta}=15$ mK, and, with the assumption of only an acoustic phonon exchange, a value of about 10 mK is found for the total quadrupolar coefficient, G^{δ}. Obviously since G^{μ} varies as $(B^{\mu})^2$, i.e., as α_J^2 from one compound to another, the values determined here, although larger, show the same trend as the ones observed in $TbPO_4$ ($G^{\gamma}=7$ mK and $G^{\delta}=70$ mK).[7] Note that the difference between the values for the two symmetries comes from the elastic constant C_0^{δ}, which is five times smaller than C_0^{γ} in the R zircon series.

All these couplings are too small to drive an ordering of the corresponding order parameter owing to the Van Vleck behavior of the first-order magnetic susceptibility as well as of the strain susceptibilities, χ_{γ} and χ_{δ}. In particular, χ_{δ} is very small and the temperature variation of χ_{δ}^{-1} exhibits a minimum around 13 K, which corresponds to an overly large G^{δ} critical value of 350 mK. For the γ symmetry, the χ_{γ}^{-1} variation also has a minimum at 13 K with a 8.4 mK critical value, larger than the observed one. As previously stated the extremum of the strain susceptibilities is due to the quadrupolar nature of the first excited doublet. By analogy to the case of $TmPO_4$,[22] it could be speculated that a magnetic field may suppress the Van Veck behavior and restore a quadrupolar ordering. We have checked that in such a situation, which is just the present case of level crossing, the Zeeman term overwhelms any other interactions and enforces a simple

polarized magnetic phase.

Although the Ho^{3+} system remains undercritical, the large sensitivity of the first excited doublet to γ quadrupolar coupling, illustrated by the fact that the χ_γ strain susceptibility is much larger than the χ_δ one, is confirmed by the study of Ho-doped $DyVO_4$ and $TbVO_4$ crystals. The $DyVO_4$ and $TbVO_4$ lattices are known to distort at $T_D = 14$ K (Ref. 23) and at $T_D = 33$ K,[24] where the dominant couplings are, respectively, $\gamma(B_{1g})$ and δ (B_{2g}). The γ quadrupolar field in $DyVO_4$ splits the Ho^{3+} first excited doublet by 14.5 cm^{-1} at 7 K, an order of magnitude more than any other doublet in the Ho^{3+} spectrum. Its response to the δ quadrupolar field in $TbVO_4$ is clearly smaller, although the quadrupolar temperature, thus the quadrupolar field are at their maximum.

The level crossing at 11.4 T has been thoroughly studied as a function of temperature. To our knowledge, such a magnetization jump of about $8\mu_B$ has never been observed in the paramagnetic phase. Its general description starting from the CEF is quite good with however two unexplained features; the high-field magnetization and the field width of the crossing. The $0.2\mu_B$ overestimation of the high-field magnetization is particularly hard to understand since the calculated moment does not drastically depend on reasonable shifts of the CEF or of the G^α coefficient from their most likely values. Second, it is possible that the two-step nature of the crossing revealed at low temperature may be explained in terms of mechanical stresses in the clamped sample, although the symmetric nature of the transition seems somewhat unlikely by chance alone. The coexistence of the two features may lead one to suscept other origins in addition to mechanical stresses, such as, for instance, the existence of inequivalent $4f$ sites. This hypothesis may be supported by electric susceptibility measurements in the neighboring compound $DyVO_4$, which reveals an anomalous increase of the dielectric constant along the c axis near the Jahn-Teller transition.[25] This increase was understood as a possible consequence of the onset of an antiferroelectric ordering, driven by the softening γ strain mode. Thus complementary studies of the static and dynamic physical properties near the level crossing, as well as in the temperature range of the broadening of the first excited doublet may be fruitful.

To summarize our results on $HoVO_4$, the CEF from Ref. 9 is confirmed, with very small modifications to fit our magnetic susceptibility data. This has allowed us to describe the spectroscopic, magnetic and magnetoelastic properties. The magnetoelastic coefficients have been determined by the extented susceptibility formalism in order to consistently analyze the third-order magnetic susceptibility, parastriction, and elastic constant measurements for the different symmetry lowering modes, which have then been compared with analogous determinations in $TbPO_4$. The magnetoelastic modulations of the CEF are very similar in these two compounds, which belong to different series and the strengths of the quadrupolar couplings are also comparable with the occurrence of a Jahn-Teller transition for a given rare earth essentially depending on the characteristics of the low-lying levels, i.e., on the CEF in association with the P, V, or As element. This comparison constitutes the first coherent analysis of the large family of R zircons, for which a great variety of magnetic and magnetoelastic properties of which seems to be ruled essentially by the CEF. Ongoing studies in other isomorphous systems will allow us to confirm this picture.

The most interesting peculiarity of $HoVO_4$ is the level crossing induced by a magnetic field along the c axis. The transition field as well as the $8\mu_B$ magnetization jump have been described in detail. The two-step nature of the transition is intriguing, especially if, as we have suggested, its origin might be other than a by-product of mechanical stresses acting within the sample.

ACKNOWLEDGMENTS

[1]W. G. Wyckoff, *Crystal Structure* (Interscience, New York, 1965), Vol. 3, p. 15.

[2]G. A. Gehring and K. A. Gehring, Rep. Prog. Phys. **38**, 1 (1975).

[3]P. Morin and D. Schmitt, in *Ferromagnetic Materials,* edited by K. H. J. Buschow and E. P. Wohlfarth (North-Holland, Amsterdam, 1990), Vol. 5, p. 1.

[4]P. Morin, J. Rouchy, and D. Schmitt, Phys. Rev. B **37**, 5401 (1988).

[5]P. Morin and J. A. Blanco, J. Magn. Magn. Mater. **119**, 59 (1993).

[6]P. Morin and J. Rouchy, Phys. Rev. B **48**, 256 (1993).

[7]P. Morin, J. Rouchy, and Z. Kazei, Phys. Rev. B **50**, 12 625 (1994).

[8]J. E. Battison, A. Kasten, M. J. M. Leask, and J. B. Lowry, J.

Phys. C **10**, 323 (1977).

[9]B. Bleaney, J. F. Gregg, P. Hansen, C. H. A. Huan, M. Lazzouni, M. J. M. Leask, I. D. Morris, and M. R. Wells, Proc. R. Soc. London, Ser. A **416**, 63 (1988).

[10]B. Bleaney, F. H. N. Robinson, and M. R. Well, Proc. R. Soc. London Ser. A **362**, 179 (1978).

[11]B. Bleaney, Physica **69**, 317 (1973).

[12]H. Suzuki, N. Nambudripad, B. Bleaney, A. L. Allsop, G. J. Bowden, I. A. Campbell, and N. J. Stone, J. Phys. (Paris) Colloq. **39**, C6-800 (1978).

[13]H. Suzuki, T. Ohtsuka, S. Kawarazaki, N. Kunitomi, R. M. Moon, and R. M. Nicklow, Solid State Commun. **49**, 1157 (1984).

[14]B. Bleaney, Proc. R. Soc. London Ser. A **370**, 313 (1980).

[15]T. Goto, A. Tamaki, T. Fujimura, and H. Unoki, J. Phys. Soc.

Jpn. **55**, 1613 (1986).

[16]K. H. J. Stevens, Proc. Phys. Soc. A **65**, 209 (1952).

[17]E. du Trémolet de Lacheisserie, Ann. Phys. **5**, 267 (1970).

[18]R. L. Melcher, in *Physical Acoustics,* edited by W. P. Mason and R. N. Thurston (Academic, New York, 1976), Vol. **XII**, p. 1.

[19]P. M. Levy, P. Morin, and D. Schmitt, Phys. Rev. Lett. **42**, 1417 (1979).

[20]H. Bischoff, B. Pilawa, A. Kasten, and H. G. Kahle, J. Phys. Condens. Matter **3**, 10 057 (1991).

[21]S. I. Andronenko, A. N. Bazhan, V. A. Ioffe, and Yu. P. Udanov, Sov. Phys. Solid State **27**, 379 (1985).

[22]B. G. Vekhter, V. N. Golubev, and M. D. Kaplan, JETP Lett. **45**, 169 (1987).

[23]A. H. Cooke, C. J. Ellis, K. A. Gehring, M. J. M. Leask, D. M. Martin, B. M. Wanklyn, M. R. Well, and R. L. White, Solid State Commun. **8**, 689 (1970).

[24]R. J. Elliot, R. T. Harley, W. Hayes, and S. R. P. Smith, Proc. R. Soc. London, Ser. A **328**, 217 (1972).

[25]H. Unoki and T. Sakudo, Phys. Rev. Lett. **38**, 137 (1977).